This is the author's version of an article that has been published in this journal. Changes were made to this version by the publisher prior to publication.
The final version of record is available at http://dx.doi.org/10.1109/LMWC.2015.2409989

Kink Effect in S_{22} for GaN and GaAs HEMTs

Giovanni Crupi, *Senior Member, IEEE*, Antonio Raffo, *Member, IEEE*, Alina Caddemi, *Member, IEEE*, and Giorgio Vannini, *Member, IEEE*

***Abstract*—This letter provides a clear understanding of the kink effect in S_{22} for active solid-state electronic devices. The origin of the kink effect is ascribed to the intrinsic section of the transistor, whereas the extrinsic elements determine its shape at the extrinsic ports. Therefore, to fairly compare the kink effect for GaN and GaAs HEMTs, the present analysis is not only focused on the whole devices but also on their intrinsic sections. The experimental evidence shows that, independently of the specific semiconductor technology, the size and the frequency band of the kink effect are mainly due to the values of the intrinsic transconductance and capacitances, respectively.**

***Index Terms*—kink effect, equivalent circuit, GaAs, GaN, HEMT, scattering parameter measurements.**

I. Introduction

THE kink effect (KE) in the output scattering parameter (S_{22}) has shown to affect transistors based on different semiconductor technologies (e.g., GaAs, GaN, and Si) [1]-[8]. This phenomenon is caused by the transition of the output impedance (Z_{out}) from a low-frequency series resistor-capacitor (RC) circuit to a high-frequency parallel RC circuit. Circuit designers should properly take the KE into account, especially for the design of broadband output matching networks [5], [6]. The KE can be described in terms of equivalent circuit elements, since the appearance and shape of the KE can be interpreted as a result of their combined effects. Therefore, to identify the circuit elements playing the dominant role, several studies have been developed over the years and different results have been reported. Nevertheless, the origin of the KE has been mainly attributed to high values of g_m [1]. In line with this theory, GaN HEMTs are strongly affected by the KE, since high g_m values are typical for this technology suitable for high-power applications [9]-[11].

Recently, a set of parameters has been defined to study the KE in terms of the concavity change of $Im(S_{22})$ versus $Re(S_{22})$ by using the second derivative D2 [7]. In particular, the size of the KE has been quantified with the parameter called kink size (KS), which is given by the negative peak value of D2 occurring at the kink frequency point (KFP). Furthermore, the kink frequency band (KFB), i.e., the frequency range between the onset and the disappearance of the KE, has been defined as the band delimited by the two frequencies where D2 becomes zero, namely the lower and upper limits of the KFB (KFBL and KFBU). Trustworthy values of this set of parameters cannot be calculated directly from D2 of the measurements because of the high sensitivity to noise of the second derivative. To overcome this drawback, model simulations may be used to achieve a smooth behavior of D2. In previous studies, model simulations based on an equivalent circuit have been used for GaAs HEMTs with different gate widths [7], while and an artificial neural network (ANN) approach has been used for a GaN HEMT [8]. Although the ANNs allow obtaining a smooth behavior of S_{22}, the circuit extraction is needed to access the intrinsic section and to interpret the kink parameters in terms of the circuit elements. The present study has been based on equivalent circuit simulations not only for the GaAs but also for the GaN HEMTs to compare the impact of the KE in S_{22} for both types of devices and in particular for their intrinsic sections. The de-embedding of the extrinsic contributions allows making easier the interpretation of the KE by shifting closer to its origin that is inherently rooted in the intrinsic section, whereas the extrinsic elements tend to mask the KE. The importance of investigating the intrinsic device comes from that fact that, as the technology progresses, the extrinsic contributions should be minimized as much as possible to maximize the device performance. Hence, the potential performance of the GaAs and GaN technologies can be effectively compared only by analyzing the intrinsic sections. Furthermore, most of the extrinsic parameters represent those parasitic contributions arising from the interconnections between the actual transistor and the outside world (e.g., contact pads and access transmission lines), which only exist in device measurements based on off-wafer calibration but not in real applications. Therefore, even if the KE can be absent in the measurements, it can still appears when the actual transistor is used for real circuit applications. In light of that, the investigation of the KE for the intrinsic section of the device is a mandatory task to assist device technologists and circuit designers. The present analysis shows for the first time that, independently of the investigated technology, the kink size and the kink frequency parameters should be mainly ascribed to the values of the intrinsic transconductance and capacitances, respectively.

This work was supported by the project PON 01_01322 PANREX with financial support by Italian MIUR and 'HF Circuits' project.

G. Crupi and A. Caddemi are with the DICIEAMA, University of Messina, 98166 Messina, Italy (e-mail: crupig@unime.it).

A. Raffo and G. Vannini are with the Department of Engineering, University of Ferrara, 44122 Ferrara, Italy.

II. Experimental Results

The behavior of S_{22} is analyzed for two AlGaN/GaN HEMTs on SiC substrate. The first device has a gate length of

Copyright (c) 2015 IEEE. Personal use is permitted. For any other purposes, permission must be obtained from the IEEE by emailing pubs-permissions@ieee.org.

This is the author's version of an article that has been published in this journal. Changes were made to this version by the publisher prior to publication.
The final version of record is available at http://dx.doi.org/10.1109/LMWC.2015.2409989

0.7 µm and a gate width of 2x400 µm (device A), while the second device has a gate length of 0.25 µm and a gate width of 8x50 µm (device B). Furthermore, S_{22} has been also studied for a GaAs HEMT with a gate length of 0.15 µm and a gate width of 10x60 µm. For convenience and ease of comparison, Table I presents a summary of the values of KS, KFBL, KFP, KFBU, KFB, g_m, C_{gs}, C_{gd}, C_{ds}, and f_T (i.e., $f_T = g_m/(2\pi(C_{gs}+C_{gd}))$) for the three tested devices. The kink parameters are not reported for the whole GaN device B, since the KE appears only for the intrinsic device.

Fig. 1 illustrates the KE in S_{22} for the GaN device A: whole (blue) and intrinsic (red) devices with V_{DS} = 10 V (a) and V_{DS} = 20 V (b). As can be clearly seen, the KE is reduced by increasing V_{DS} from 10 V to 20 V. This result can be attributed to the reduction of g_m from 253 mS to 223 mS. This g_m degradation is caused by the more severe heating phenomena under higher dissipated power, which is increased from 2.4 W (V_{DS} = 10 V) to 4.4 W (V_{DS} = 20 V). Furthermore, the KE becomes more pronounced after removing contributions of the extrinsic elements. This is because the KE is inherently rooted in the intrinsic device, whereas the extrinsic contributions tend to mask and reduce this effect. By mathematically removing the extrinsic contributions from the experimental data, the magnitude of KS increases from 10.5 to 22.5 at V_{DS} = 10 V and from 6.4 to 13.4 at V_{DS} = 20 V.

The behavior of S_{22} for the GaN device B is reported in Fig. 2(a). The KE is not visible in S_{22} of the whole device, whereas it appears for the intrinsic device with KS reaching a magnitude of 3.1. Therefore, the extrinsic contributions can cause the KE to disappear completely. This result is of great importance because circuit designers should be aware if the device is affected by the KE to take it into account. A clear example is the power amplifier design based on engineering the current and voltage time-domain waveforms at the intrinsic section to optimize the device performance [12].

Fig. 2(b) shows that, similarly to the case of the GaN devices, the GaAs HEMT exhibits a more pronounced KE after removing the extrinsic contributions. As a consequence, the magnitude of KS is increased from 11.2 to 22.1.

The comparison of the KE for GaAs and GaN HEMTs is a challenging task, since a comparison between devices based on different technologies, materials, and geometrical dimensions is not really straightforward. In addition, an off-wafer LRM calibration with alumina substrate has been performed for both GaN devices, whereas an on-wafer TRL calibration has been performed for the GaAs device. Hence, the calibration has moved the electrical reference planes closer to the actual device for the GaAs device with respect to the GaN ones. However, the comparison becomes feasible at the intrinsic sections, where the inconsistencies due to the different extrinsic access lay-out and calibration procedures disappear. At the intrinsic sections, similar values of KS are achieved by analyzing operating conditions with a similar value of g_m. In particular, KS is roughly equal to -22 for both the GaN device A with a g_m of 253 mS and the GaAs device with a g_m of 255 mS. This outcome definitely confirms that, independently of the tested technology, the origin of the KE and its size have to be mainly ascribed to g_m. This result is in accordance with previous experimental studies showing that the magnitude of KS increases at the operating conditions (e.g., temperature, gate width, and bias point) leading to higher g_m values [7], [8].

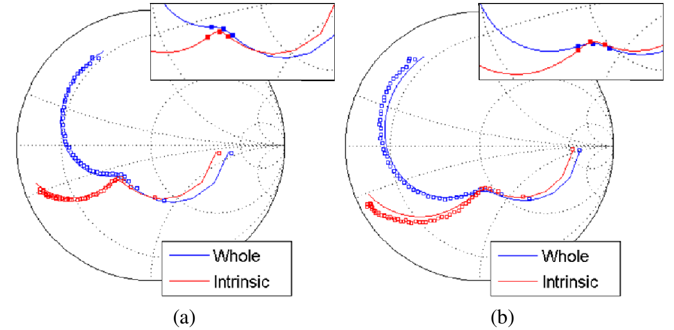

(a) (b)

Fig. 1. Measured (symbols) and simulated (lines) S_{22} from 40 MHz to 40 GHz for the GaN device A at V_{GS} = -2 V: whole (blue) and intrinsic devices (red) with V_{DS} = 10 V (a) and V_{DS} = 20 V (b). The inset highlights the KE with three squares at the calculated KFBL, KFP, KBFU in the simulated S_{22}.

TABLE I. KINK SIZE, LOWER LIMIT OF THE KINK FREQUENCY BAND, KINK FREQUENCY POINT, UPPER LIMIT OF THE KINK FREQUENCY BAND, KINK FREQUENCY BAND, GM, CGS, CGD, CDS, F_T FOR TESTED HEMTS

DEVICE	*KS*	*KFBL (GHz)*	*KFP (GHz)*	*KFBU (GHz)*	*KFB (GHz)*	*g_m (mS)*	*C_{gs} (pF)*	*C_{gd} (pF)*	*C_{ds} (pF)*	*f_T (GHz)*
Whole GaN device A V_{DS}=10V, V_{GS}=-2V	-10.5	2.0	3.2	5.4	3.4	253	2.43	0.25	0.36	15.0
Intrinsic GaN device A V_{DS}=10V, V_{GS}=-2V	-22.5	1.8	3.0	5.8	4.0					
Whole GaN device A V_{DS}=20V, V_{GS}=-2V	-6.4	1.6	2.8	4.6	3.0	223	2.52	0.17	0.29	13.2
Intrinsic GaN device A V_{DS}=20V, V_{GS}=-2V	-13.4	1.6	3.0	5.0	3.4					
Intrinsic GaN device B V_{DS}=10V, V_{GS}=-2.72V	-3.1	5.5	8.5	13.3	7.8	90	0.55	0.09	0.17	22.4
Whole GaAs device V_{DS}=6V, V_{GS} -0.6V	-11.2	5.9	9.7	16.6	10.6	255	0.70	0.07	0.13	52.7
Intrinsic GaAs device V_{DS}=6V, V_{GS}=-0.6V	-22.1	5.6	10.9	17.8	12.2					

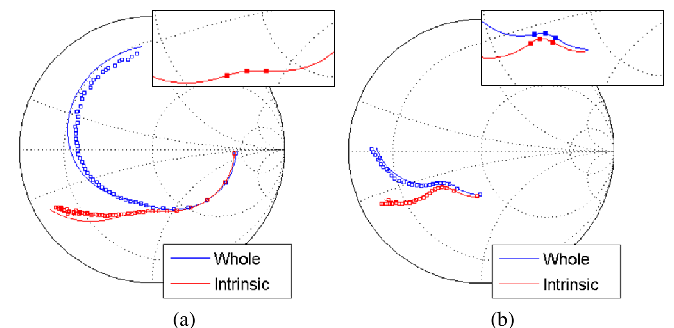

(a) (b)

Fig. 2. Measured (symbols) and simulated (lines) S_{22} for the GaN device B at V_{GS} = -2.72 V, V_{DS} = 10 V, and the frequency going from 0.1 GHz to 50 GHz (a) and for the GaAs HEMT at V_{GS} = -0.6 V, V_{DS} = 6 V, and the frequency going from 2.5 GHz to 65 GHz: whole (blue) and intrinsic devices (red). The inset highlights the KE with three squares at the calculated KFBL, KFP, KBFU in the simulated S_{22}.

Copyright (c) 2015 IEEE. Personal use is permitted. For any other purposes, permission must be obtained from the IEEE by emailing pubs-permissions@ieee.org.

This is the author's version of an article that has been published in this journal. Changes were made to this version by the publisher prior to publication.
The final version of record is available at http://dx.doi.org/10.1109/LMWC.2015.2409989

As introduced in [1], the KE can be associated to the transition of Z_{out} from a low-frequency series RC circuit (i.e., $Z_{out} = r + (j\omega C_s)^{-1}$) to a high-frequency parallel RC circuit (i.e., $Y_{out} = g + j\omega C_p$). By disregarding the intrinsic non-quasi-static effects, which play a significant role only at high frequencies, and omitting R_{ds}, which merely changes the starting point of S_{22} without affecting the KE, a simplified expression of Z_{out} and Y_{out} can be obtained in terms of g_m, C_{gs}, C_{gd}, C_{ds} [1]:

$$Z_{out} = \left(\frac{Z_0}{1+g_m Z_0} + \frac{g_m}{(Y_0+g_m)^2} \frac{C_{gs}}{C_{gd}} \right) \left(\frac{(1+g_m Z_0)C_{gd}}{(1+g_m Z_0)C_{gd}+C_{ds}} \right)^2 + \frac{1}{j\omega\left[(1+g_m Z_0)C_{gd}+C_{ds}\right]} \quad (1)$$

$$Y_{out} = \left[Y_0 \left(\frac{C_{gd}}{C_{gs}+C_{gd}} \right)^2 + \frac{g_m C_{gd}}{C_{gs}+C_{gd}} \right] + j\omega \left(\frac{C_{gs} C_{gd}}{C_{gs}+C_{gd}} + C_{ds} \right) \quad (2)$$

where Y_0 is the reciprocal of Z_0 (i.e., 50 Ω).

The effects of C_{gs}, C_{gd}, C_{ds} on r and g cancel each other as far as they change by the same factor and thus g_m is the dominant element in determining the size of the KE. In particular, higher g_m leads to a more pronounced KE by decreasing r and increasing g. On the other hand, it should be pointed out that larger capacitances imply that the transition from Z_{out} to Y_{out} is achieved at lower frequencies by increasing C_s and C_p. In accordance with this statement, similar values of KFBL, KFP, and KFBU are obtained for the GaN device B and the GaAs device, since they have similar values of the intrinsic capacitances. Finally, it should be noticed that, although the degradation of g_m at higher V_{DS} leads to a much smaller KS for the GaN device A, only minor variations of KFBL, KFP, and KFBU are achieved since the intrinsic capacitances change only slightly with V_{DS}.

It should be pointed out that the KE affects the device performance at operating frequencies of interest, since KFP is much lower than f_T. As a matter of fact, microwave transistors have a wide range of possible applications at frequencies well below f_T in order to obtain a high gain. On the other hand, KFP is significantly higher than the cut-off of the low-frequency dispersion (i.e., in the megahertz range). Therefore, we may rule out that the KE is caused by traps and thermal effects, which play a crucial role for microwave transistors, especially for the GaN technology, by impacting their performance and even reliability [13-15]. These non equilibrium processes cannot follow the applied signal at high frequencies, since their time constants are much longer than the reciprocal of microwave frequencies. Nevertheless, low-frequency phenomena can affect the quiescent bias condition and, in turn, also the RF behavior as it is dependent on the DC bias point. Hence, low-frequency dispersion can affect the KE as its size and shape are due to the combined effect of the circuit elements and their values depend on the DC bias point. It should be underlined that the origin of the KE can be mainly correlated to the relatively high value of the RF g_m, which can be heavily influenced by the low-frequency dispersion.

III. Conclusions

The kink effect in S_{22} has been deeply studied for HEMTs fabricated in both GaN and GaAs technologies. It has been shown that the intrinsic transconductance and capacitances are mainly responsible for the size and frequency band of the kink effect, respectively. Furthermore, it has been demonstrated that the extrinsic contributions can mask the kink effect to cause even its disappearance.

References

[1] S.-S. Lu, C. Meng, T.-W. Chen, and H.-C. Chen, "The origin of the kink phenomenon of transistor scattering parameter S_{22}," *IEEE Trans. Microw. Theory Techn.*, vol. 49, no. 2, pp. 333-340, Feb. 2001.

[2] H.-Y. Tu, Y.-S. Lin, P.-Y. Chen, S.-S. Lu, and H.-Y. Pan, "An analysis of the anomalous dip in scattering parameter S_{22} of InGaP-GaAs heterojunction bipolar transistors (HBTs)," *IEEE Trans. Electron Devices*, vol. 49, no. 10, pp. 1831-1833, Oct. 2002.

[3] Y.-S. Lin and S.-S. Lu, "An analysis of small-signal gate–drain resistance effect on RF power MOSFETs," *IEEE Trans. Electron Devices*, vol. 50, no. 2, pp. 525-528, Feb. 2003.

[4] Y.-S. Lin, "An analysis of small-signal source-body resistance effect on RF MOSFETs for low-cost system-on-chip (SoC) applications," *IEEE Trans. Electron Devices*, vol. 52, no. 7, pp. 1442-1451, Jul. 2005.

[5] J. Shohat, I. D. Robertson, and S. J. Nightingale, "Investigation of drain-line loss and the S_{22} kink effect in capacitively coupled distributed amplifiers," *IEEE Trans. Microw. Theory Techn.*, vol. 53, no. 12, pp. 3767-3773, Dec. 2005.

[6] H. Gao, X. Sun, Y. Hua, X. Zhang, R. Wang, and G. P. Li, "A composite transistor to suppress kink phenomenon in HBTs for broadband design," *IEEE Electron Device Lett.*, vol. 31, no. 10, pp. 1113-1115, Oct. 2010.

[7] G. Crupi, et al., "The kink phenomenon in the transistor S_{22}: a systematic and numerical approach," *IEEE Microw. Wireless Comp. Lett.*, vol. 22, no. 8, pp. 406-408, Aug. 2012.

[8] G. Crupi, et al., "An extensive experimental analysis of the kink effects in S_{22} and h_{21} for a GaN HEMT," *IEEE Trans. Microw. Theory Techn.*, vol. 62, no 3, pp. 513-520, Mar. 2014.

[9] P. M. Cabral, J. C. Pedro, and N. B. Carvalho, "Nonlinear device model of microwave power GaN HEMTs for high power-amplifier design," *IEEE Trans. Microw. Theory Techn.*, vol. 52, no. 11, pp. 2585-2592, Nov. 2004.

[10] A. Ramadan, T. Reveyrand, A. Martin, J.-M. Nebus, P. Bouysse, L. Lapierre, J.-F. Villemazet, and S. Forestier, "Two-stage GaN HEMT amplifier with gate-source voltage shaping for efficiency versus bandwidth enhancements," *IEEE Trans. Microw. Theory Techn.*, vol. 59, no. 3, pp. 699-706, Mar. 2011.

[11] H. Jang, P. Roblin, and Z. Xie, "Model-based nonlinear embedding for power-amplifier design," *IEEE Trans. Microw. Theory Techn.*, vol. 62, no. 9, pp. 1986-2002, Sep. 2014.

[12] A. Raffo, F. Scappaviva, and G. Vannini, "A new approach to microwave power amplifier design based on the experimental characterization of the intrinsic electron-device load line," *IEEE Trans. Microw. Theory Techn.*, vol. 57, no. 7, pp. 1743-1752, Jul. 2009.

[13] G. Meneghesso, M. Meneghini, A. Tazzoli, N. Ronchi, A. Stocco, A. Chini, and E. Zanoni, "Reliability issues of gallium nitride high electron mobility transistors," *Int. J. Microw. Wirel. Technol.*, vol. 2, no. 1, pp 39-50, Feb. 2010.

[14] A. M. Darwish, H. A. Hung, A. A. and Ibrahim, "AlGaN/GaN HEMT with distributed gate for channel temperature reduction," *IEEE Trans. Microw. Theory Techn.*, vol. 60, no. 4, pp 1038-1043, Apr. 2012.

[15] D. W. Runton, B. Trabert, J. Shealy, and R. Vetury, "History of GaN: High-power RF gallium nitride (GaN) from infancy to manufacturable process and beyond," *IEEE Microw. Mag.*, vol. 4, no. 3, pp 82-93, May 2013.

Copyright (c) 2015 IEEE. Personal use is permitted. For any other purposes, permission must be obtained from the IEEE by emailing pubs-permissions@ieee.org.

View publication stats